

A parametric study of Trombe walls for passive cooling of buildings

Guohui Gan

Institute of Building Technology, Department of Architecture and Building Technology, University of Nottingham, University Park, Nottingham, UK

Received 18 March 1997; accepted 2 April 1997

Abstract

Air movement in a naturally-ventilated room can be induced through the use of a solar chimney or Trombe wall. In this work Trombe walls were studied for summer cooling of buildings. Ventilation rates resulting from natural cooling were predicted using the CFD (computational fluid dynamics) technique. The renormalization group (RNG) $k-\epsilon$ turbulence model was used for the prediction of buoyant air flow and flow rate in enclosures with Trombe wall geometries. The CFD program was validated against experimental data from the literature and very good agreement between the prediction and measurement was achieved. The predicted ventilation rate increased with the wall temperature and heat gain. The effects of the distance between the wall and glazing, wall height, glazing type and wall insulation were also investigated. It was shown that in order to maximize the ventilation rate, the interior surface of a Trombe wall should be insulated for summer cooling. This would also prevent undesirable overheating of room air due to convection and radiation heat transfer from the wall. © 1998 Elsevier Science S.A.

Keywords: Air movement; Solar chimney; Trombe wall; Computational fluid dynamics technique; Renormalization group $k-\epsilon$ turbulence model

1. Introduction

Passive solar heating has increasingly been used internationally in the last two decades. Even in the UK solar energy has been utilized for space heating. However, summer overheating is often a problem in many passive solar houses due to excessive south-facing glazing [1]. This problem can be alleviated by shading, for example, but in buildings with internal heat sources a better approach to tackle the problem without using mechanical means may lie in making use of solar energy to increase air movement indoors through a

Trombe wall or solar chimney. Passive solar heating has been widely studied but very few studies have been carried out for passive solar cooling.

A Trombe wall is a south-facing concrete or masonry wall blackened and covered on the exterior by glazing. The massive thermal wall (storage wall) serves to collect and store solar energy. The stored energy is transferred to the inside building for winter heating or facilitates room air movement for summer cooling. Fig. 1 shows operations of a Trombe wall for heating and cooling. In the heating mode, air enters the space between the wall and glazing from the bottom vent

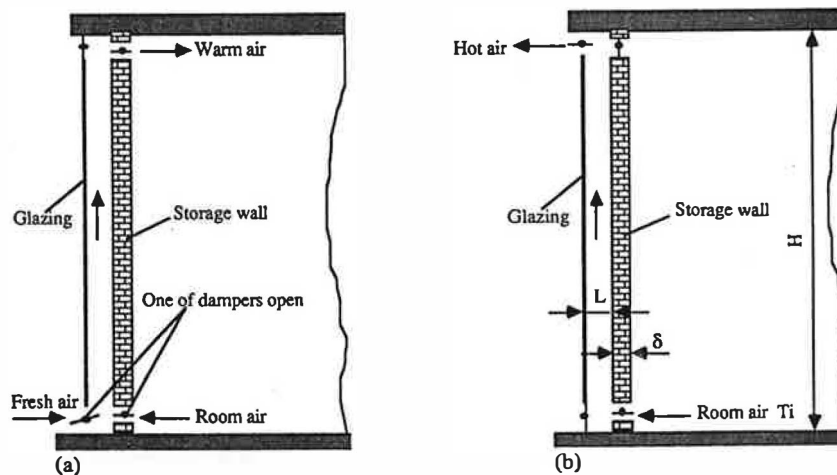


Fig. 1. Schematic diagram of Trombe wall for (a) winter heating and (b) summer cooling.

either opened to the living room when outdoor air is cold or to the ambient when the outdoor temperature is moderate, for example, $> 10^{\circ}\text{C}$. The air is heated up by the wall and flows upwards due to the buoyancy effect. It then returns to the living space through the top vent. For summer cooling, dampers are so positioned that the buoyancy forces generated by the solar heated air between the warm wall and glazing draws room air to the bottom vent and outdoor air into the room through open windows or vents in other exterior walls. The heated air flows out to the ambient rather than into the living space through the top vent. Depending on the ambient temperature, this operation can be either for daytime ventilation or night cooling. In hot regions where the outdoor air during the day is often hot, ventilation for sensible cooling is not feasible but the storage wall still provides a good thermal insulation to heat flow into the room. During the night, air movement induced by the warm Trombe wall draws the cool ambient air into the space and removes heat from the interior of the building. In regions with a temperate climate such as in the UK, the summer outdoor air temperature is generally not very high and indoor air can be warmer than outdoor air due to high heat loads through lighting and other electrical sources, solar gains and occupants. The wall can be used for ventilation cooling during daytime to reduce or eliminate the need for energy intensive refrigerative cooling. In both heating and cooling operations, the heat input into the room or ventilation rate can be controlled by adjusting the air flow through dampers.

Energy and air movement in the channel of a Trombe wall is induced by natural convection. The effect of channel width on natural convection between vertical parallel plates was studied experimentally by Sparrow and Azevedo [2]. They found that heat transfer was reduced dramatically if the width of the channel had the same order of magnitude as the boundary layer thickness. For a typical building to avoid flow blockage effects, the channel width should be greater than 4.7 cm [3]. Sandberg and Moshfegh [4] performed experiments on the channel flow using two vertical parallel walls heated from one side. The relation between the measured air flow rate and heat flux rate was found to follow a power law. They also used a numerical method to study the effects of heat flux rate and channel width on the convective heat transfer in the channel [5]. The flow rate through the channel was found to increase with decreasing channel aspect ratio, i.e. increasing channel width. This was attributed to the decreasing wall frictional resistance with increasing channel width. The width of the channel was also found to influence the surface temperature of the insulated wall but not the temperature of the heated wall.

Solar chimneys have been investigated by a number of researchers for providing a comfortable living environment in buildings. Barozzi et al. [6] conducted experimental tests on a 1:12 scale model of solar chimney. The results were then used to validate a 2-D laminar flow simulation model. Bansal et al. [7] analytically studied a solar chimney coupled with a wind tower to induce natural ventilation. It was estimated

that the effect of a solar chimney was relatively much higher for lower wind speeds. Bouchair [8] experimentally and theoretically studied the performance of a typical cavity used as a solar chimney in inducing ventilation into a house. Measurements of air temperature and velocity were made on a full-scale model under steady-state conditions. Importance was placed on the cavity width and air inlet area. It was observed that the mass flow rate maximized when the cavity width was between 0.2 and 0.3 m. With a 0.1 m wide cavity, the inlet height was found to have no effect on the mass flow rate but when the cavity width was increased to 0.3 and 0.5 m, the mass flow rate increased with the inlet height. Besides, the mass flow rate was found to increase with increasing surface temperature.

Most investigations on Trombe walls have so far been concerned with winter heating. Warrington and Ameel [9] carried out experiments in a scaled test facility of a Trombe wall geometry. The effects of Trombe wall non-isothermality, aspect ratios, and opening sizes on heat transfer, fluid temperature distributions and flow patterns were examined. It was found that Nusselt numbers increased slightly as the mass transfer openings in the Trombe wall were increased but increasing the opening sizes caused an increased thermal stratification in the living space. Pitts and Craigen [10] described a technique for controlling air flow through Trombe walls. The technique involved the use of a low power axial flow fan activated by a controller in accordance with the air temperature in Trombe walls or with reference to room conditions. Du and Bilgen [11] numerically investigated the influence of openings and non-uniform heat generation on the heat transfer in a modified Trombe wall with a porous medium used as an absorber. Borgers and Akbari [12] numerically studied free convective turbulent flow within a Trombe wall for a wide range of channel geometries, relative surface temperatures and flow rates. They then developed correlations for estimating the performance of Trombe walls. However, at that time measured data for flows in Trombe wall geometries were not available for validating the numerical method and so the correlations had limited applications. Recently computational fluid dynamics (CFD) has been used [13,14] to simulate the air flow and heat transfer in a Trombe wall coupled to a room. In these simulations, constant wall temperature conditions were used to investigate the potential of Trombe walls for summer ventilation. In practice, Trombe walls which are designed mainly for winter heating are non-insulated and so for daytime summer ventilation the wall temperature is not only non-isothermal but unknown. It will be shown that insulation of the storage wall has a considerable effect on the wall temperature and ventilation rate of the system. Therefore, using heat gains is a more realistic approach to optimization of the design of Trombe walls.

The purpose of the present study is to use CFD to simulate a Trombe wall for summer ventilation with solar heat gains and conduction heat transfer. A CFD program is first validated against experimental data for enclosures with Trombe wall geometries. Numerical investigation is then carried out

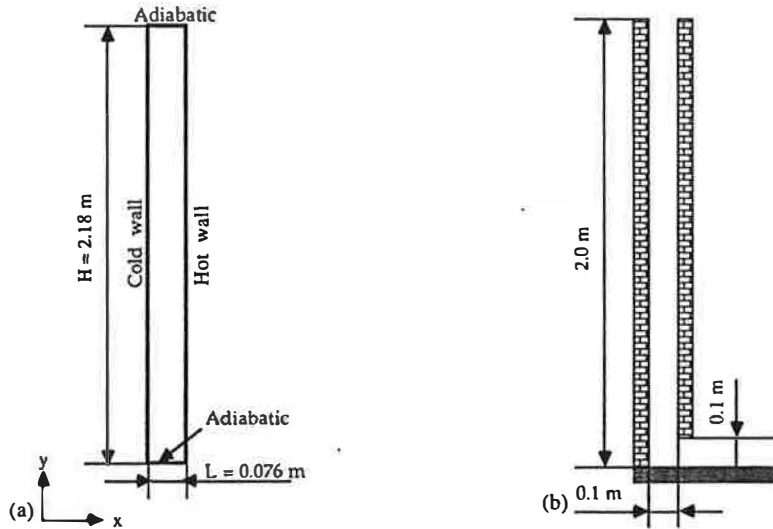


Fig. 2. Dimensions of the elevation of (a) tall cavity and (b) solar chimney.

into parameters that influence the performance of a Trombe wall such as the channel width and height, heat gains and wall insulation.

2. Methodology

The CFD technique was used for air flow simulation in enclosures. The air flow model consisted of a system of governing equations representing continuity, momentum, turbulence, enthalpy and concentration. Air turbulence was represented by the renormalization group (RNG) turbulence model developed by Yakhot and Orszag [15]. For an incompressible steady-state flow the time-averaged air flow equations can be written in the following form

$$\frac{\partial}{\partial x_i}(\rho U_i \phi) + \frac{\partial}{\partial x_i} \left(\Gamma_\phi \frac{\partial \phi}{\partial x_i} \right) = S_\phi \quad (1)$$

where ϕ represents the mean velocity component U_i in x_i direction, turbulent parameters and mean temperature, Γ_ϕ is the diffusion coefficient and S_ϕ is the source term for variable ϕ .

Details of the model equations are described in Ref. [16]. Based on the two-dimensional finite-volume TEAM code [17], the governing equations are solved for the three-dimensional Cartesian system using the SIMPLE algorithm and the Power-Law differencing scheme [18].

Validation of the program was performed by comparing the predictions with the experimental results for turbulent natural convection in a tall cavity by Betts and Bokhari [19] and in a solar chimney by Bouchair [8]. Fig. 2 shows the elevation of the cavity and chimney.

2.1. Tall cavity

The internal dimensions of the cavity were 2.18 m high, 0.076 m wide and 0.52 m deep. Temperatures of cold left and

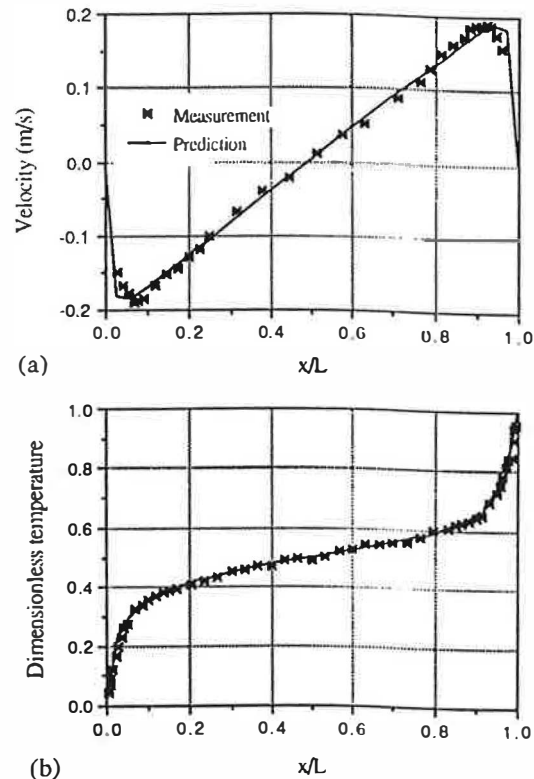


Fig. 3. Comparison of predicted and measured (a) air velocity and (b) temperature at the cavity mid-height.

hot right walls were controlled at $T_c = 15^\circ\text{C}$ and $T_h = 55^\circ\text{C}$, respectively. Other walls were insulated. Air velocities in the cavity were measured using a laser Doppler anemometry system. Thermocouples were used for temperature measurement.

Fig. 3 shows a comparison between the predicted and measured air velocity and temperature (T_n) profiles at the cavity mid-height. As seen from the figure, the predicted velocity profile agrees closely with the measured results. The predicted dimensionless temperature $(T_n - T_c)/(T_h - T_c)$ is also in excellent agreement with the measurement.

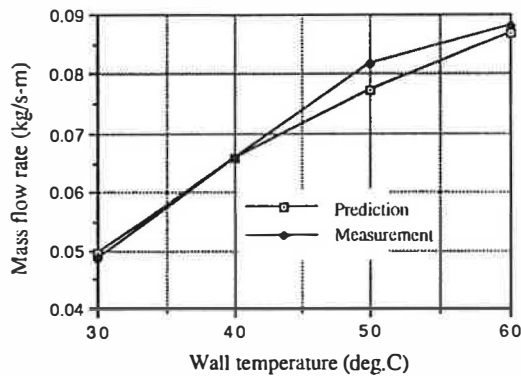


Fig. 4. Comparison of the predicted and measured mass flow rate in the chimney.

2.2. Solar chimney

The chimney was 2 m high, 3 m long and of variable width. The inlet height also varied in the experiment. Validation was performed for the inlet height and channel width of 0.1 m. All the wall faces were heated by electric heaters to the same controlled temperature from 30 to 60°C. The inlet air temperature was controlled at 20°C. Temperatures were measured with copper–constantan thermocouples. The speed of air movement was measured with a heated thermistor anemometer and air flow patterns were observed with the use of smoke.

Fig. 4 shows the predicted and measured mass flow rates per unit length of the chimney. It is seen that good agreement between the prediction and measurement is again achieved. The average difference between the predicted and measured flow rates is about 2%; the maximum difference is 5% at the wall temperature 50°C. The predicted mass flow rate increases with wall temperature according to

$$\dot{m} = 0.0197\Delta T^{0.4015} \quad (r = 1.00) \quad (2)$$

where \dot{m} is the mass flow rate per unit length ($\text{kg s}^{-1} \text{m}^{-1}$) and ΔT is the difference in temperature between the wall surface and inlet air (K).

Sandberg and Moshfegh [4] found that for a channel heated from one side the relation between the flow rate and heat input followed a power law with an exponent of about 0.4. The present prediction confirms their finding.

These two sets of comparisons demonstrate that the computer code can be used to study the air flow in enclosures with Trombe wall geometries.

3. Parametric study of a Trombe wall

Numerical simulation was carried out for a Trombe wall system for summer ventilation in the UK with various conditions. As a base simulation, the storage wall was assumed to be 2.4 m high and 0.3 m thick. It was made of dense concrete with thermal conductivity of $1.4 \text{ W m}^{-1} \text{ K}^{-1}$. The glazing was a 6 mm plate glass with absorptivity for direct

solar radiation of 0.08. The distance between the glazing and wall was 0.1 m. The width of the inlet and outlet openings was also 0.1 m.

Since the wall temperature was unknown, the heat flux was taken as a boundary condition. The wall solar heat gain was calculated from the daily mean total solar irradiance and mean solar gain factor on July 23. The daily mean outdoor air temperature was 19°C [20]. The daily mean solar irradiance on south wall was 165 W m^{-2} and mean solar gain factor for single glazing was 0.76. Hence, the wall heat gain was 125.4 W m^{-2} . The room air temperature was assumed at 20°C.

The length of the system was large compared with the width and so it was taken as a two-dimensional configuration.

The predicted effects of varying conditions for the Trombe wall and ambient are discussed later.

3.1. Channel width

The effect of channel width on the predicted air flow rate is shown in Fig. 5. It is seen that for a fixed inlet and outlet size of 0.1 m in width, the flow rate was almost unaffected by the channel width. This is because the total pressure loss through the system was mainly caused by the entrance and exit losses. The pressure loss due to friction in the channel decreased with the increase of channel width but the variation of friction loss was small compared with pressure losses in the openings. The predicted mean surface temperature for the heated wall with 0.1 m inlet width varied within a small range between 35.8 and 36.5°C. Thus, the effect of channel width on the wall temperature was negligible. This agrees with predictions for heat transfer between two parallel walls by Moshfegh and Sandberg [5]. In their predictions, however, the two ends of a channel were fully open and so the air flow rate increased with the channel width. For the inlet slot of 0.1 m wide, experimental data for solar chimney [8] also showed that the effect of channel width on the flow rate was small for a wall temperature of 30°C but the effect could be significant when the wall temperature was increased to say 60°C. For the Trombe wall simulated here, when the total solar irradiance was increased to 340 W m^{-2} and the corresponding wall heat gain to 258.4 W m^{-2} , the predicted wall surface tem-

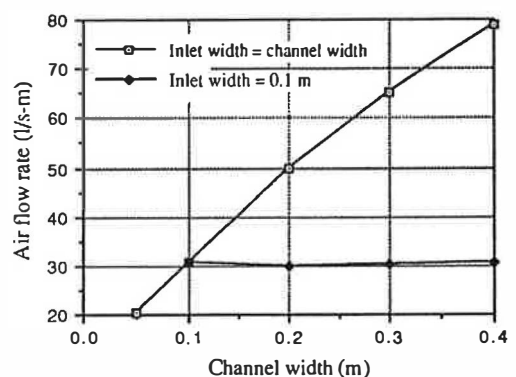


Fig. 5. Effect of channel width on the air flow rate (wall solar heat gain = 125.4 W m^{-2}).

Table 1
Solar heat gains of the Trombe wall system

Total solar irradiance (W m^{-2})	20.0	55.0	90.0	165.0	210.0	340.0	450.0	550.0
Wall solar heat gain (W m^{-2})	15.2	41.8	68.4	125.4	159.6	258.4	342.0	418.0
Heat gain by glazing (W m^{-2})	1.6	4.4	7.2	13.2	16.8	27.2	36.0	44.0

perature was increased to between 48.5 and 49.9°C. However, the predicted air flow rate for channel widths from 0.1 to 0.4 m varied still only in a small range between 41.6 and 43.0 $\text{l s}^{-1} \text{m}^{-1}$. This can be attributed to the higher pressure loss at the exit of the Trombe wall than that of the solar chimney as is discussed later. As a result, the variation of the ratio of friction loss to entrance and exit pressure losses for the Trombe wall is smaller than that for the solar chimney. This led to the negligible effect of channel width on the flow rate for the Trombe wall even at high wall temperatures.

When the width of the inlet and outlet openings was set to be the same as the channel width, i.e., constant cross-section from the inlet to outlet openings, the flow rate increased with the channel width. This is due to the increased opening area for air flow. In contrast, for a given amount of heat input, increasing the flow rate resulted in the reduced air temperature gradient along the channel, thus reducing the buoyancy effect and mean air velocity. For example, the mean air velocity at the inlet opening decreased from 0.3 m s^{-1} for 0.1 m opening width to 0.2 m s^{-1} for 0.4 m opening width. With constant cross-section from the inlet to outlet openings and wall solar heat gain of 125.4 W m^{-2} , the air flow rate is related to the channel width by the following equation:

$$Q = 143.4L^{0.6582} \quad (r = 1.00) \quad (3)$$

where L is the channel width (m) and Q is the air flow rate per unit length ($\text{l s}^{-1} \text{m}^{-1}$).

3.2. Wall heat gain

The effect of wall solar heat gain was investigated using total solar irradiance at different sun times (up to 550 W m^{-2} corresponding to the noon sun time for the south face and the corresponding wall solar heat gain of 418 W m^{-2}). Table 1 presents the wall solar heat gains for the investigation. The outdoor air temperature under different sun times would deviate from the daily mean value. However, for comparison, the outdoor and indoor air temperatures were kept constant at 19 and 20°C, respectively. Fig. 6 shows that the predicted flow rate increased with increasing wall heat gain. The mean wall temperature also increased with the heat gain but the increment was not linear due to the conductive heat loss through the wall. The effects of wall heat gain on the wall temperature and air flow rate can be described by the following correlations:

$$T_w = T_i + 0.2395q^{0.8667} \quad (r = 1.00) \quad (4)$$

$$Q = 4.5725q^{0.4015} \quad (r = 0.99) \quad (5)$$

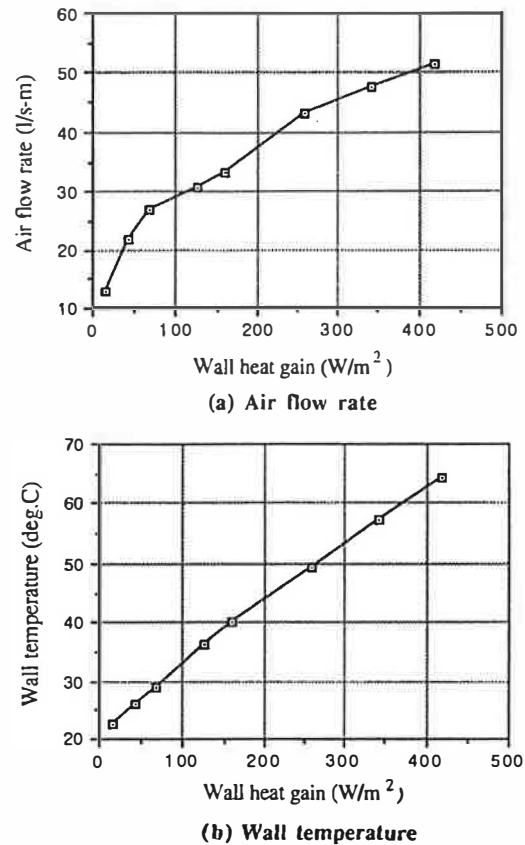


Fig. 6. Effect of wall heat gain on the air flow rate.

where q is the wall heat gain (W m^{-2}), T_i is the inlet (room) air temperature ($^{\circ}\text{C}$) and T_w is the mean temperature of the wall surface facing the glazing ($^{\circ}\text{C}$).

3.3. Wall height

The height of storage wall affects the total buoyancy force and hence flow rate. The effect of wall height on the predicted flow rate is shown in Fig. 7. By comparing Fig. 6 with Fig. 7, it is seen that the flow rate for a 3 m high wall with 125.4 W m^{-2} heat gain is the same as that for a 2.4 m high wall with 219 W m^{-2} heat gain ($Q = 39.8 \text{ l s}^{-1} \text{m}^{-1}$). Therefore, an increase in wall height by a quarter is equivalent to an increase of wall heat gain by three quarters. The relationship between the flow rate and wall height between 2.4 and 4.0 m follows a square root law:

$$Q = 17.84[(H - 2.28)]^{1/2} + 24.86 \quad (r = 1.00) \quad (6)$$

where H is the height of storage wall (m).

The square root law agrees with the general stack effect for natural ventilation [20].

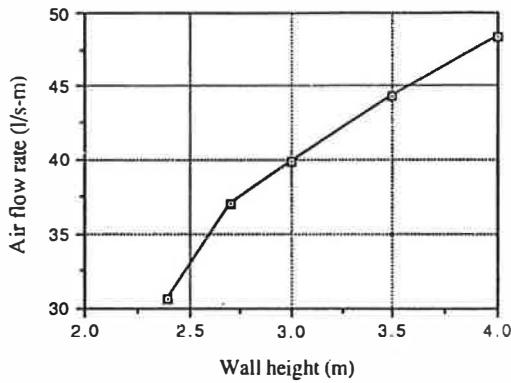


Fig. 7. Effect of wall height on the air flow rate.

3.4. Thermal insulation

The insulation levels of glazing and storage wall influence the surface temperatures and thereby the flow rate. To investigate the influence of glazing insulation on the flow rate, predictions were performed for the Trombe wall with double glazing (25 mm air space). Because of the dependence of the solar gain factor on the type of glazing, two values of the wall solar heat gain were used: (i) calculated from the solar gain factor for double glazing = 105.6 W m^{-2} (corresponding to the same total solar irradiance); and (ii) taken as the value for single glazing = 125.4 W m^{-2} (corresponding to the same wall heat gain). The difference between them was taken as an additional solar heat absorbed by the double glazing unit (33 W m^{-2} in total). The predicted air flow rates were $34.0 \text{ l s}^{-1} \text{ m}^{-1}$ for the same total solar irradiance and $35.9 \text{ l s}^{-1} \text{ m}^{-1}$ for the same wall heat gain. Hence, using double glazing could increase the flow rate by 11% to 17%.

The thickness of storage wall is an important parameter affecting the performance and its optimum value is determined principally on the basis of the required heat capacity to keep the fluctuations of wall temperature within limits. Under steady-state conditions, the thickness of a non-insulated wall affects the thermal resistance and consequently the air flow rate. When the thickness increases, the surface temperature of the wall facing the glazing increases and so does the buoyancy effect. Fig. 8 shows the effect of wall thickness on the wall temperature and air flow rate. The predicted wall temperature and air flow rate can be correlated as functions of wall thickness in the range of 0.1 to 1.0 m as follows:

$$T_w = T_i + 21.3 + 4.03 \ln \delta \quad (r = 1.00) \quad (7)$$

$$Q = 34.1 + 2.95 \ln \delta \quad (r = 1.00) \quad (8)$$

or in terms of thermal resistance:

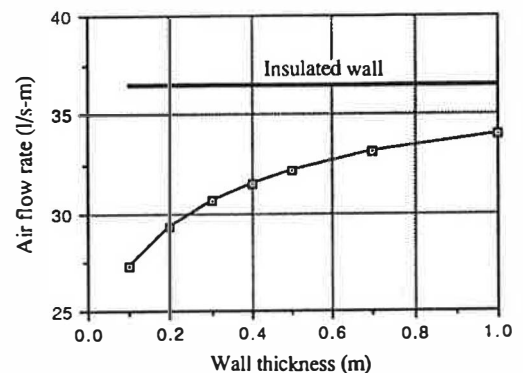
$$T_w = T_i + 22.6 + 4.03 \ln R \quad (r = 1.00) \quad (9)$$

$$Q = 35.1 + 2.95 \ln R \quad (r = 1.00) \quad (10)$$

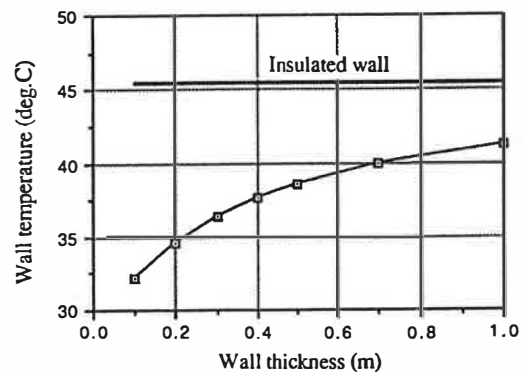
where δ is the thickness of storage wall (m) and R is the thermal resistance of the wall ($\text{m}^2 \text{ K W}^{-1}$), obtained by dividing the thickness by the thermal conductivity.

When the interior surface of the storage wall is insulated, equivalent to an infinitely thick wall, the wall heat gain is fully utilized for generating buoyancy forces. For the simulated wall, insulating the interior surface led to increases of wall surface temperature by 9 K (from 36.3 to 45.4°C) and flow rate by 19% (from 30.6 to 36.5 $\text{l s}^{-1} \text{ m}^{-1}$). The increased flow rate is equivalent to the increase of heat gain of the wall without insulation (given by Eq. (5)) by approximately 40%. In other words, about 40% wall heat gain would be transferred to the living room by conduction through a non-insulated wall of 0.3 m thick. When the insulated wall was used with double glazing, the predicted flow rate was further increased to $40.0 \text{ l s}^{-1} \text{ m}^{-1}$ under the same total solar irradiance.

These predictions indicate that for summer cooling insulating the interior surface of the storage wall is more effective than increasing the thermal resistance of glazing. Besides, when the storage wall is insulated, excessive overheating due to south-facing glazing can be avoided. For winter heating, increasing the thermal resistance of glazing is generally more advantageous as this reduces the heat loss through glazing while making use of conductive heat transfer from the storage wall to the living room. However, Baker [21] showed that in the UK non-insulated Trombe walls using only conductive heat gains were not viable for passive heating. From this study, therefore, it can be concluded that for applications in a climate similar to the UK the interior surface of Trombe walls should be insulated for summer cooling as well as



(a) Air flow rate



(b) Wall temperature

Fig. 8. Effect of wall thickness on the air flow rate.

winter heating. To make the system more effective, double glazing should also be employed.

3.5. Opening position

The flow path near the exit in a Trombe wall differs from that in a solar chimney. In a solar chimney, the heated air ejects straight to the atmosphere whereas the air in a Trombe wall often exits through one or more restricted openings on the glazing side or storage wall. As a result, the flow in a Trombe wall near the exit has to turn a right angle from the channel and in addition involves abrupt contraction at the entrance of the exit opening, thus incurring additional pressure losses. For the same thermal conditions of the Trombe wall with a channel width of 0.1 m, when the exit opening was assumed at the top of the channel to simulate the chimney exhaust, the predicted flow rate per unit length was increased by one third from 30.6 to 41.2 l s⁻¹. Hence, when only cooling is required, a solar chimney is preferable to a Trombe wall. Besides, the chimney height is not restricted to the level of building wall height, providing flexibility in the system design in order to make full use of the stack effect.

4. Conclusions

The study shows that the computer code developed can be used for the prediction of buoyant air flow and flow rate in enclosures with Trombe wall geometries.

When a Trombe wall is used for summer cooling, the ventilation rate induced by the buoyancy effect increases with the wall temperature, solar heat gain, wall height and thickness. Provided that the dimensions of the inlet and outlet openings increases with channel width, the ventilation rate also increases with the distance between the wall and glazing. The use of double glazing instead of single glazing for a Trombe wall system not only reduces heat losses in winter but also enhances passive cooling in summer. To maximize the ventilation rate for summer cooling, the interior surface of the storage wall should be insulated. This also prevents undesirable overheating of room air due to convection and radiation heat transfer from the wall.

If solar energy is used for passive cooling only, a solar chimney is preferable to a Trombe wall.

References

[1] G.S. Yakubu, The reality of living in passive solar homes: a user experience study, *Renewable Energy*, 8 (1996) 177.

- [2] E.M. Sparrow and L.F.A. Arzvedo, Vertical channel natural convection spanning between the fully developed and the single-plate boundary-layer limit, *Int. J. Heat Mass Transfer*, 28 (1985) 1847.
- [3] R. Anderson and F. Kreith, Natural convection in active and passive solar thermal systems, *Advances in Heat Transfer*, 18 (1985) 1.
- [4] M. Sandberg and B. Moshfegh, Investigation of fluid flow and heat transfer in a vertical channel heated from one side by PV elements, Part II—Experimental study, *Renewable Energy*, 8 (1996) 254.
- [5] B. Moshfegh and M. Sandberg, Investigation of fluid flow and heat transfer in a vertical channel heated from one side by PV elements, Part I—Numerical study, *Renewable Energy*, 8 (1996) 248.
- [6] G.S. Barozzi, M.S.E. Imbabi, E. Nobile and A.C.M. Sousa, Physical and numerical modelling of a solar chimney-based ventilation system for buildings, *Build. Environ.*, 27 (1992) 433.
- [7] N.K. Bansal, R. Mathur and M.S. Bhandari, Study of solar chimney assisted wind tower system for natural ventilation in buildings, *Build. Environ.*, 29 (1994) 495.
- [8] A. Bouchair, Solar chimney for promoting cooling ventilation in southern Algeria, *Building Services Eng. Res. Technol.*, 15 (1994) 81.
- [9] R.O. Warrington and T.A. Ameel, Experimental studies of natural convection in partitioned enclosures with a Trombe wall geometry, *Solar Energy Eng.*, 117 (1995) 16.
- [10] A.C. Pitts and S. Craigen, A technique for controlling air flow through modified Trombe walls, *Proc. 17th Air Infiltration and Ventilation Centre Conf.—Optimum Ventilation and Air Flow Control in Buildings*, Vol. 2, Gothenberg, Sweden, 17–20 September, 1996, pp. 477–485.
- [11] Z.G. Du and E. Bilgen, Natural convection in composite wall collectors with porous absorber, *Solar Energy*, 45 (1992) 325.
- [12] T.R. Borgers and H. Akbari, Free convective turbulent flow with the Trombe wall channel, *Solar Energy*, 33 (1984) 253.
- [13] H.B. Awbi and G. Gan, Simulation of solar-induced ventilation, *Proc. 2nd World Renewable Energy Congress*, Vol. 4, Reading, UK, 13–18 September, 1992, pp. 2016–2030.
- [14] S.K. Chaturvedi, D.T. Chen and T.O. Mohieldin, Ventilation characteristics of a Trombe wall thermosyphon loop, *Proc. Int. Symp. on Room Air Conditioning and Ventilation Effectiveness*, Tokyo, Japan, July 22–24, 1992, pp. 624–631.
- [15] V. Yakhot and S.A. Orszag, Renormalization group analysis of turbulence, *J. Scientific Computing*, 1 (1986) 3.
- [16] G. Gan and S.B. Riffat, Naturally ventilated buildings with heat recovery: CFD simulation of thermal environment, *Building Services Eng. Res. Technol.*, 18 (1997) 67–75.
- [17] P.G. Huang and M.A. Leschziner, An Introduction and Guide to the Computer Code TEAM, Report TFD/83/9, Department of Mechanical Engineering, University of Manchester Institute of Science and Technology, Manchester, UK, 1983.
- [18] S.V. Patankar, *Numerical Heat Transfer and Fluid Flow*, Hemisphere, Washington, DC, 1980.
- [19] P.L. Betts and I.H. Bokhari, Experiments on natural convection of air in a tall cavity. *Proc. 5th ERCOFTA/International Association for Hydraulic Research Workshop on Refined Flow Modelling*, Vol. V, Natural Convection in Tall Cavities, Chatou, Paris, April 25–26, 1996.
- [20] CIBSE Guide Volume A, Chartered Institution of Building Services Engineers, London, 1986.
- [21] N.V. Baker, The use of passive solar gains for the pre-heating of ventilation air in houses, Report No. ETSU-S-1142, ECD Partnership, London, 1985.